ISBN: 978-3-95450-219-6 ISSN: 2226-0366 doi: 10.18429/JACoW-LINAC2024-TUPB100

DESIGN OF A 25 kW FUNDAMENTAL POWER COUPLER FOR CONDUCTION COOLED NB3SN INDUSTRIAL LINAC*

S. U. Thielk†, R. Agustsson, S. Kutsaev, A. Pronikov, A. Martinez
RadiaBeam LLC, Santa Monica, CA, USA
J. Vennekate, G. Ciovati, R. Rimmer
Thomas Jefferson National Accelerator Facility, Newport News, VA, USA

Abstract

RadiaBeam has designed a 915 MHz, 25 kW CW Fundamental Power Coupler (FPC) to power a Nb3Sn coated superconducting radio-frequency (SRF) cavity. Unlike traditional FPCs for SRF cavities, the device relies only on conductive cooling by cryocoolers. The baseline design was adapted from the liquid helium cooled 805 MHz SNS FPC with the notable addition of an intermediate 50 K thermal intercept and associated RF shield. Engineering design details to address the thermomechanical, manufacturability, and structural challenges will be presented. Particular emphasis will be placed on static and dynamic heat load management along with finite element analysis to validate mechanical stability. Additionally, initial manufacturing studies of the coaxial window brazing will be discussed.

INTRODUCTION

The design complexity of an FPC is rooted in the strict vacuum, thermal and mechanical requirements while ensuring the manufacturing complexity and risk is minimized. Further, these efforts must be performed iteratively with RF design to ensure efficient power coupling into a cavity. Although this paper is not focused on RF design, it is pertinent to note that the FPC is designed to operate at 915 MHz with a S11 = -50.17 dB, S21 = -.006 dB and a Q-factor between 2.96e6 to 3.3e6 with the intended Nb3Sn coated SRF cavity. Similar to the SNS approach [1], a doorknob transition and coaxial style window were used.

A key requirement of the FPC is to transition from cryogenic temperatures near the cavity to the room temperature cryostat while minimizing the heat load to the cooling systems. In addition to the static heat transfer, heat generated from RF losses and radiation must be accounted for. SRF cavities fabricated from pure niobium operate around 2 K, typically achieved with complex and costly liquid helium systems. Nb3Sn coated SRF cavities can operate with low losses at ~4 K, permitting the use of cryocoolers and conduction based heat removal. Without the option to route liquid helium near the FPC to cavity connection, a 50 K intercept linked to the first stage of the cryocooler can be employed. In this effort, the required heat loads were defined as <2 W and <50 W to the SRF cavity and to the 50 K intercept, respectively. All of these factors make FPC design a multi-disciplinary effort as documented elsewhere in more comprehensive design overviews [2, 3].

* The work was supported by U.S. Department of Energy, Office of Science, Office of Nuclear Physics via a grant from the Accelerate Innovations in Emerging Technologies program and by DOE-ARDAP via a grant from the Accelerator Stewardship program. The contribution from JLab is based upon work supported by the U.S. Department of Energy, Office of Science, Office of Nuclear Physics under contract DE-AC05-06OR23177
† sthielk@radiabeam.com

MECHANICAL DESIGN

The FPC fabrication can be divided into three primary sub-assemblies as shown in Fig. 1: the doorknob, window, and outer conductor. The doorknob is responsible for transferring power from a WR975 rectangular waveguide into a coaxial port for the FPC. It consists of a welded aluminum box containing the copper doorknob and inner and outer conductor extensions. The window sub-assembly serves as the atmosphere to vacuum barrier, includes the critical fixed length antenna, and provides diagnostic ports. The positioning of the antenna tip is critical to the power coupling. Therefore, there are clear advantages to include methods to adjust the position. However, a fixed length antenna was elected as the most effective approach after comparing system requirements to manufacturing complexity. The outer conductor assembly connects the flange bolted to the cavity to the window and cryostat wall. The temperature gradient across the outer conductor sub-assembly components is accomplished by a thin-walled thermal choke and an RF shield.

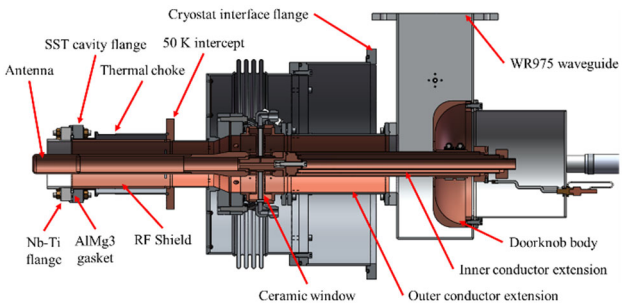

Figure 1: Cross-section of complete FPC assembly highlighting key features.

The RF shield concept was inspired by multiple publications [4- 6]. Serving as the outer conductor starting at the 50 K intercept, there is a small gap between the end of the shield and the 4.2 K cavity flange, as shown in Fig. 2. Eliminating this conduction path funnels heat from RF losses close to the cavity to the higher capacity 50 K cryocooler circuit. A small lip was added to the tip of the shield, maintaining the effectiveness while alleviating concerns about manufacturability and potential interference.

ISBN: 978-3-95450-219-6 ISSN: 2226-0366 doi: 10.18429/JACoW-LINAC2024-TUPB100

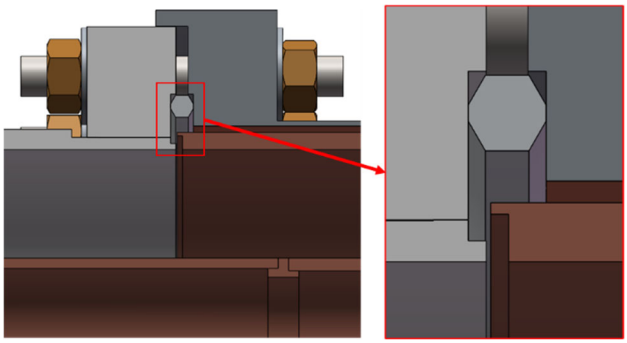

Figure 2: Cross section and detail view of RF shield choke.

The three primary sub-assemblies are independent and can be fabricated in parallel and sequentially integrated into the cryostat during final assembly. Assembly sequence, tool access, and cable routing for instrumentation were a major consideration during the design process. As demonstrated in Fig. 3, most of the connections are made on the back side of the window assembly prior to doorknob installation. This includes an RF probe, two full range inverted magnetron vacuum gages, two sapphire viewports, two polyimide backed heaters to prevent condensation, and a spare port without a pre-designated use. Lastly, an SHV feedthrough is installed on the doorknob housing to allow voltage biasing of the inner conductor.

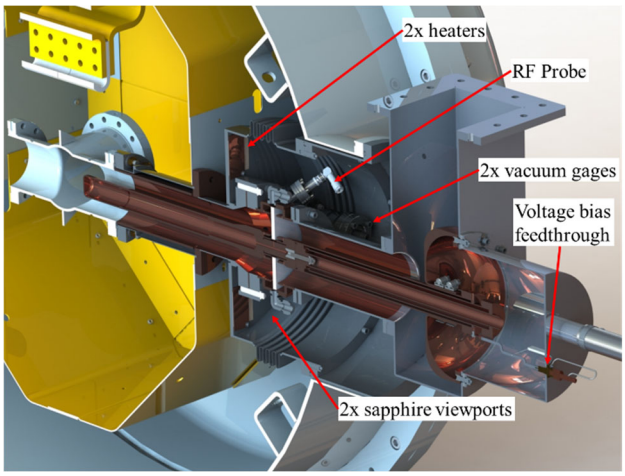

Figure 3: Cross-section depicting the installed FPC and instrumentation components.

MECHANICAL SIMULATIONS

All simulations were performed in ANSYS Mechanical under room temperature conditions and cross checked against Solidworks Simulation results. The properties for fully annealed copper and stainless steel were used since all components will be subjected to high temperature vacuum braze cycles. All braze and weld joints were considered fully bonded and the properties of the braze alloy itself were ignored. Models were simplified by removing details such as edge breaks, small gaps for part fitment and braze shims. For meshing, the global maximum element size was set to 2 mm. A 0.25 mm max element size mesh control was added to the thin wall of copper brazed to the inner diameter of the ceramic.

Antenna Deflection

A simulation was performed to investigate the deflection of the antenna due to gravity. The results show a maximum deflection of 0.033 mm at the antenna tip. The corresponding stress plot shows a maximum stress of 11.10 MPa located at the braze interface between the window and inner conductor, which is approximately one third of the yield strength of annealed copper. Both values were considered safe and acceptable.

Vacuum Forces

An analysis of the impact of vacuum forces was conducted (Fig. 4). The primary areas of interest were the ceramic window, thin wall thermal choke, and antenna internal volume. The results indicate safe ranges of stress for all areas of interest. A maximum of 82.24 MPa occurs on the large cryostat vacuum barrier plate, providing a safety factor greater than 2x when compared to the yield strength of annealed stainless steel.

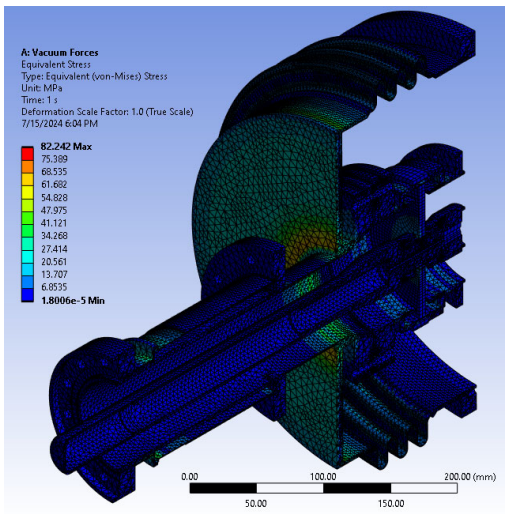

Figure 4: Von mises stress plot showing vacuum force effects.

Modal Analysis

A simulation was run to satisfy the >60 Hz fundamental frequency requirement. Given the complexity of the mechanical interfaces with the SRF cavity, cryostat, thermal intercepts and waveguide, it was decided to fix the air side outer conductor window flange as the only boundary condition. The result was a 114 Hz fundamental frequency, with the antenna tip oscillating transverse to its axis, meeting the requirement.

Impulse Analysis

A series of simulations were run to assess the impact of a 5 G acceleration impulse on the assembly. The results are shown in Table 1. The scenario of interest is when the FPC is installed in the cryostat perpendicular to gravity and then subjected to shipping or seismic disturbances. Unlike the other simulations, the ceramic inner diameter braze joint was modelled as a 0.25 mm fillet filling the space generated by a chamfer on the ceramic. This was integrated after

ISBN: 978-3-95450-219-6 ISSN: 2226-0366 doi: 10.18429/JACoW-LINAC2024-TUPB100

initial simulations showed excessive stress concentration at the sharp corner interface between the ceramic and copper. In addition to a static 5 G load, transient simulations were run with the acceleration applied as a half sine pulse at four time scales, 10 ms, 25 ms, 50 ms and 100 ms. The maximum stress was consistently located on the vacuum side braze joint fillet between inner conductor and ceramic. The values of the maximum stress slightly exceeded the yield strength of annealed copper (33 MPa) for all scenarios. This indicates that most of the deformation is elastic and would be recovered in the unloaded condition.

Table 1: Simulation Results of 5 G Acceleration Impulse

Time Scale	Max Stress (MPa)	Max Deformation (mm)
10 ms	48.5	.15
25 ms	37.8	.11
50 ms	35.5	.11
100 ms	33.9	.10
Static	33.9	.10

Thermomechanical

A thermomechanical simulation was performed to understand how the location of the antenna tip changes when the assembly is installed and cooled to cryogenic temperatures. The results showed that the tip of the antenna moves 0.33 mm closer to the beamline. Manufacturing tolerances are expected to be of similar magnitude and when combined still provide comfortable safety within the ± 1.5 mm positioning requirement. Nonetheless, the room temperature model was adjusted accordingly.

THERMAL SIMULATIONS

Thermal simulations in ANSYS with RF loss data imported from CST Studio were performed to ensure the design conformed to the heat load requirements to the cavity and 50 K circuit of the cryocooler. Temperature dependent thermal conductivities were accounted for, but electrical conductivities were constant room temperature values, erring conservatively.

Since the cross section of the cavity port was used as the 4.2 K boundary condition, the accuracy of the adjacent conduction paths was critical. The electron beam weldment of the Nb cavity port and the NbTi cavity flange were modeled as 2 mm penetrations at both front and back of the engaged length. A 0.05 mm gap was maintained in the trapped volume of the unwelded length. Additionally, two conductive pathways were accounted for between the NbTi cavity flange and stainless steel cavity flange on the FPC. First, contact between studs, washers, nuts and flanges. Secondly, the AlMg3 gasket, which was modeled to have a 0.9 mm wide contact surface on both sealing faces. This amount of flattening of the hexagonal cross section was derived from empirical data for similarly sized AlMg3 hexagonal gaskets [7]. To stay conservative, no contact resistance was built into the model. The results are shown in Fig. 5 and Table 2, demonstrating conformance to the design requirements.

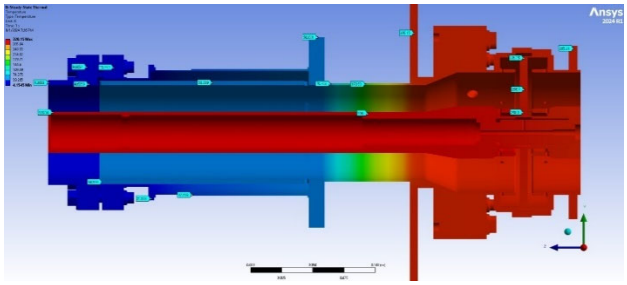

Figure 5: Temperature map of thermal simulations.

Table 2: Heat Loads to Cryocooler Broken Down by Source for 25 kW Forward Power

	Static load (W)	Radiation load (W)	RF heat load (W)	Total heat load (W)
4.2 K	0.62	0.06	0.39	1.07
50 K	19.39	0.16	1.78	21.33

BRAZE STUDY

One of the critical and challenging aspects of fabricating an FPC is brazing the ceramic window that forms the vacuum barrier between the cavity and coaxial RF power transmission line. To confirm the design feasibility, a test braze was conducted (Fig. 6). For consistency with the FPC design, Morgan Advanced Materials AL300, 97.6% purity alumina was chosen for the study, representative of the FPC design. Copper sleeves with thin walls at the braze joints were machined and custom tooling was used to ensure appropriate joint gaps at braze temperatures.

Braze alloy was visible around the entire circumference of both braze joints. Helium leak checking using a rubber seal demonstrated a leak rate of 8.9 x 10^{-10} mbar*L/sec with no reaction when the surround area was flooded with helium.

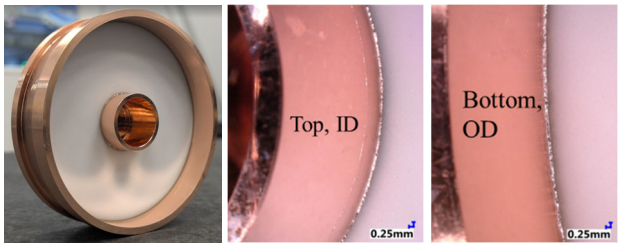

Figure 6: (left) Test braze assembly after brazing; (middle, right) detail images of braze joint.

CONCLUSION

The design for a low heat-leak 915 MHz FPC has been completed. With the implementation of an RF shield and fixed length antenna, the design meets all thermal and mechanical requirements. After successful demonstration of the ceramic brazing, fabrication of the device is planned for 2025.

ACKNOWLEDGEMENTS

The authors would like to thank Tom Schultheiss of TJS Technologies for the helpful discussion.

ISBN: 978-3-95450-219-6 ISSN: 2226-0366 doi: 10.18429/JACoW-LINAC2024-TUPB100

REFERENCES

[1] Y. Kang *et al.,* "RF Processing of Couplers for the SNS Superconducting Cavities", in *Proc. 12th Int. Workshop on RF Superconductivity,* Ithaca, NY, USA, July 2005, paper THP49, pp. 577-579.

[2] I. E. Campisi, "Fundamental Power Couplers for Superconducting Cavities", in *Proc. The 10th Workshop on RF Superconductivity (SRF '01)*, Tsukuba, Japan, Sep. 2001, paper FA005, pp. 132-143.

[3] USPAS, https://uspas.fnal.gov/materials/08UMD/Couplers.pdf

[4] S. Kazakov, "How to eliminate a copper coating and to increase average power of main coupler", in *Proc. 15th Int. Conf. on RF Superconductivity (SRF '11),* Chicago, IL, USA, July 2011, paper TUPO009, pp. 368-370.

[5] R. C. Dhuley *et al*., "Design of a 10 MeV, 1000 kW average power electron-beam accelerator for wastewater treatment applications", *Phy. Rev. Accel. Beams*, vol. 25, p. 041601, Apr. 2022. doi:10.1103/PhysRevAccelBeams.25.041601

[6] N. A. Stilin *et al.,* "Design of a 1.3 GHz High-Power RF Coupler for Conduction-Cooled Systems", in *Proc. 21st Int. Conf. on RF Supercond. (SRF'23)*, Grand Rapids, MI, USA, June 2023. paper MOPMB094, pp. 342-346.

[7] P. Michaelato *et al*. "2.2.1.14 MS Final Reports for new components: Cold Flanges", INFN, Milano, Italy, 2006.